Fundamental Study on Design Method of Yaw-Moment Observer for Improvement of Drivers' Comfort for Electric Vehicle

Kenta Maeda*, Hiroshi Fujimoto**, Yoichi Hori***
The University of Tokyo
5-1-5, Kashiwanoha, Kashiwa, Chiba, 227-8561 Japan
Phone: +81-4-7136-3881*, +81-4-7136-4131**, +81-4-7136-3846***
Fax: +81-4-7136-3881*, +81-4-7136-4132**, +81-4-7136-3847***
Email: maeda@hflab.k.u-tokyo.ac.jp*, fujimoto@k.u-tokyo.ac.jp**, hori@k.u-tokyo.ac.jp***

***Abstract*—Commercialized electric vehicles (EVs) at the present time are comparatively small and light. Such vehicles are sensitive to lateral wind especially at high speed, which reduces steering stability and comfortability. In this paper, Yaw-Moment Observer (YMO) is applied to improve steering stability and comfortability by reducing the effect of disturbance caused by lateral wind. Moreover, vehicle behavior can be designed freely since YMO can nominalize the vehicle yaw characteristics. Therefore the design method of YMO to improve driver comfort and ease of driving is considered. Effectiveness of the proposed method is verified with simulations and experiments. In addition, a quantitative evaluation method for evaluating steering stability is proposed.**

I. Introduction

As a solution for energy and environmental problems, electric vehicles (EVs) are getting great attention. In addition, EVs have many advantages over internal combustion engine vehicles (ICEVs) since electric motors and inverters are utilized in EV's drive systems. Their advantages can be summarized as follows [1], [2].

1) The torque response of electric motors is 100-500 times faster than that of ICEVs.
2) All wheels can be controlled independently by adopting small and high-power in-wheel motors.
3) The output torque of an electric motor can be measured accurately from the motor current.

Based on these advantages, the authors' research group has proposed control methods for anti-slip [3], motion stabilization [4] and so on.

Although commercialized EVs at the present time are comparatively small and light because of batteries' costs and mileage per charge, they are as expensive as high-class ICEVs. In general, light vehicles can easily be affected by lateral wind, which forces drivers to adjust their steering angles for preventing from getting out of the traffic lanes, and therefore reduces steering stability and comfortability. On the other hand, luxury ICEVs are heavy and have lower center of gravity, leading to stable running performance and comfort especially at high speed. In order to popularize EVs, small and light EVs are required to archive such running performance as additional value.

Fig. 1. FPEV2-Kanon.

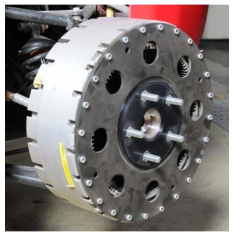

Fig. 2. In-wheel motor.

In this paper, Yaw-Moment Observer (YMO) [5] is applied to improve steering stability and comfortability by reducing the effect of disturbance caused by lateral wind. Conventional methods for improving steering stability mainly apply electric power steering (EPS) to adjust steering angle automatically [6]-[8]. The authors' research group, on the other hand, has focused on driving and braking force differences between left and right wheels, which is enabled by adopting in-wheel motors, and proposed various methods including YMO. By using YMO, yaw-moment disturbance can be detected and suppressed instantly by generating driving and braking force differences. Moreover, vehicle behavior can be designed freely since YMO can nominalize the vehicle yaw characteristics. Hence, the design method of YMO in order to improve ease of operation is considered.

In addition, a quantitative evaluation method of closed-loop test is proposed. Evaluating methods of steering stability and comfortability usually employ questionnaires on closed-loop test. However, results of such methods are dependent on individual differences, which tend to make the results vague. Therefore, in this paper, a quantitative evaluation method is suggested and its effectiveness is verified by sensory tests.

II. Experimental Vehicle

An original experimental EV "FPEV2-Kanon," which is developed by the authors' laboratory and used for performance

TABLE I
VEHICLE SPECIFICATIONS.

Vehicle Mass (m)	870 [kg]
Vehicle Inertia (I)	617.0 [kg $\cdot$ m^2]
Distance from C.G to Fromt Axle (l_f)	0.999 [m]
Distance from C.G to Rear Axle (l_r)	0.701 [m]
Front Cornering Stiffness (C_f)	12500 [N/rad]
Rear Cornering Stiffness (C_r)	29200 [N/rad]
Tread Base (d_f, d_r)	1.3 [m]
Radius of Tire (r)	0.302 [m]

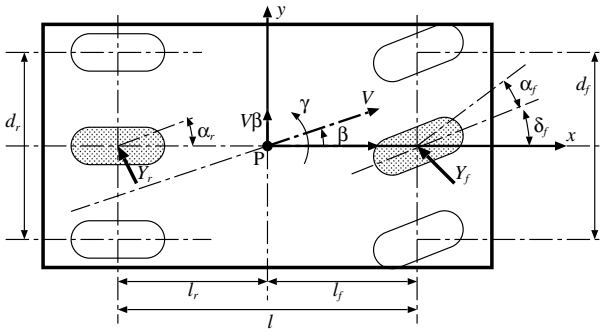

Fig. 3. Two-wheel model.

verification, is shown in Fig. 2. In this section, the characteristics of the experimental vehicle are explained.

Outer-rotor-type in-wheel motors are installed in each wheel. Since these motors adopt the direct drive system, the reaction forces from roads are directly transferred to the motors without gear reduction or backlash. The maximum torque of the front motor is ± 500 [Nm], and that of the rear one is ± 340 [Nm]. Additionally, the steering mechanism adopts active front and rear steering system by using two 250W DC motors for EPS, and they can be used for researches concerning automatic steering. The experimental vehicle's specification is shown in Table I.

III. Equations of Vehicle Dynamics

In this section, two equations that represent vehicle dynamics are explained [10]. The two-wheel vehicle model in which the characteristics of tires are regarded as the same between left and right, is used for formulating the dynamics. Fig. 3 shows the concept of the model.

If the steering angle and the wheel side-slip angle are small, the equation of vehicle lateral motion can be described as

$$\begin{aligned} & mV\left(\frac{d\beta}{dt}+\gamma\right) \\ & = -2C_f\left(\beta+\frac{l_f}{V}\gamma-\delta_f\right)-2C_r\left(\beta-\frac{l_r}{V}\gamma\right)+Y_d, \end{aligned} \tag{1}$$

where m is the vehicle mass, V is the vehicle velocity, β is the vehicle side-slip angle, γ is the vehicle yaw-rate, C_f and C_r are the cornering stiffness of front and rear wheels, δ_f is the steering angle of front wheels, l_f and l_r are the distance from the body center of gravity (i.e., C.G) to steering knuckle spindle and rear wheel axle, Y_d is the lateral force at the body center of gravity caused by disturbances such as lateral wind.

The equation of vehicle rotational motion around the yaw axis can be described as

$$\begin{aligned} I\frac{dr}{dt} &= -2C_f\left(\beta+\frac{l_f}{V}\gamma-\delta_f\right)l_f+2C_r\left(\beta-\frac{l_r}{V}\gamma\right)l_r \\ &\quad +N_z+N_d, \end{aligned} \tag{2}$$

where I is the vehicle inertia around the yaw axis, N_z is the yaw-moment generated by the torque difference between left and right in-wheel motors, N_d is the yaw-moment caused by disturbances such as lateral winds.

IV. Design Method of Yaw-Moment Observer

A. Yaw-Moment Observer

In this section, the proposed design method of Yaw-Moment Observer (YMO) to improve steering stability is explained. In (2), the yaw-moment generated by lateral forces at tires is defined as $N_t \equiv -2C_f\left(\beta+\frac{l_f}{V}\gamma-\delta_f\right)-2C_r\left(\beta-\frac{l_r}{V}\gamma\right)$, and the total yaw-moment disturbance is $N_{dt} \equiv N_t+N_d$. By these definitions, (2) is simplified as

$$I\frac{dr}{dt} = N_z + N_{dt}. \tag{3}$$

YMO is the method that estimates and compensates for N_{dt} by using disturbance observer. For frequency band less than the YMO cut-off frequency ω_c, the vehicle yaw motion is nominalized as

$$\gamma = \frac{1}{I_n s}N_{in}, \tag{4}$$

where I_n is the vehicle nominal inertia, N_{in} is the control input of the nominalized vehicle plant.

B. Proposed design method of YMO

Fig. 4 shows the block diagram of yaw-rate control using YMO. Here, K_{YMO} is the feedback gain of the observer. If $K_{\mathrm{YMO}} = 1$, Fig. 4 is nominalized into Fig. 5.

By determining the low pass filter Q and the yaw-rate feedback controller C as

$$Q = \frac{\omega_c}{s+\omega_c}, \tag{5}$$

$$C = I_n\omega_c, \tag{6}$$

the transfer function from $\hat{N}_{dt}$ to γ is described as

$$\frac{\gamma}{\hat{N}_{dt}} = \frac{1}{I_n}\frac{s}{(s+\omega_c)^2}. \tag{7}$$

I_n is the parameter that can be changed freely. (7) consists of the band-pass filter $s/(s+\omega_c)^2$ and the constant I_n^{-1}. By setting I_n high, the gain from $\hat{N}_{dt}$ to γ becomes low, namely the disturbance suppression performance is improved. This means, if I_n is set higher than the actual value I, light vehicles behave as heavy ones which are less affected by lateral winds.

Fig. 6 shows the control system block diagram for improving steering stability, which includes the driver steering angle δ_f. $G_{\gamma\delta}(s)$ is the transfer function for calculating yaw-rate

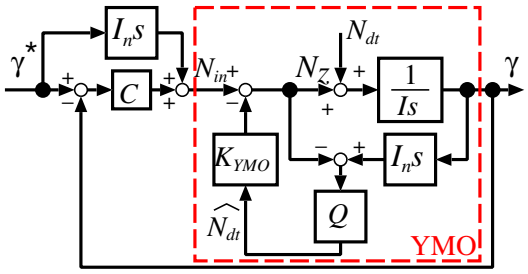

Fig. 4. Block diagram of yaw-rate control using YMO.

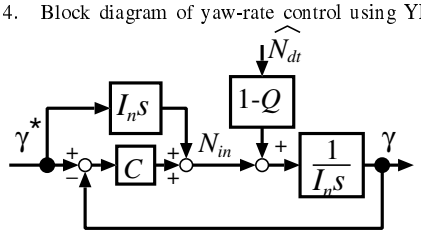

Fig. 5. Block diagram after nominalization.

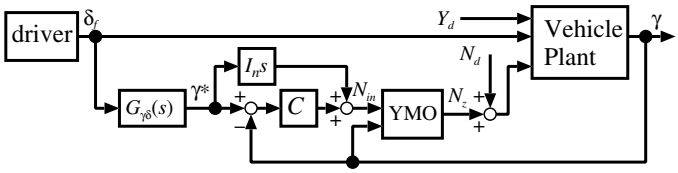

Fig. 6. Block diagram of improving steering stability control.

reference γ^* from steering angle δ_f. It can be set to a first-order lag as

$$G_{\gamma\delta}(s) = \frac{1}{1+K_s V^2} \cdot \frac{V}{l} \cdot \frac{1}{\tau_\gamma s + 1}, \tag{8}$$

where K_s is the stability factor, τ_γ is the time constant from steering angle to yaw-rate. Since vehicle yaw dynamics are nominalized by YMO, steering characteristics can be designed freely by adjusting K_s and τ_γ. For example, faster response can be realized for downtown driving by setting τ_γ low, and more stable respons can be realized for expressways by setting τ_γ high.

C. Driver model

In this section, a driver model that represents driver steering operation is employed in order to evaluate steering stability quantitatively in simulation. In this paper, a look-ahead driver model, which is simple and achieves good tracking performance to driver's target course, is used. The concept of this model is shown in Fig. 7 [10].

A driver looks forward at a distance of L, which is called look-ahead distance, and decides steering angle to decrease the difference from the target course at the looking point. ϵ is the difference between the running course and the target course at this point. Assuming that the vehicle's yaw-angle θ is small, ϵ is formulated as

$$\epsilon = y_{0L} - (y + L\theta), \tag{9}$$

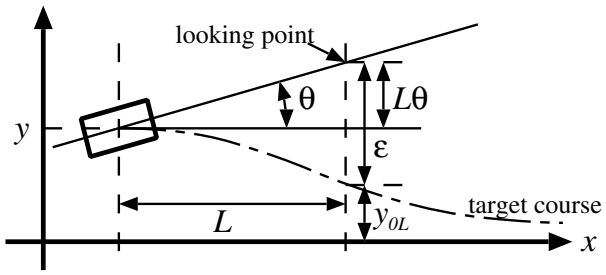

Fig. 7. Concept of look-ahead driver model.

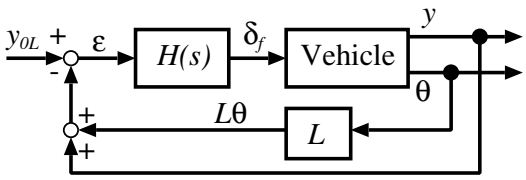

Fig. 8. Block diagram of look-ahead driver model.

where y_{0L} is the y-coordinate of the desired course at the looking point. Fig. 8 shows the driver model's block diagram, where $H(s)$ is the feedback controller of driver's operation. For simple analysis, $H(s)$ is set as one-order lag and proportion gain as

$$H(s) = h\frac{1}{\tau_L s + 1}. \tag{10}$$

The driver's lag time is set as $\tau_L = 0.3$ [s].

The look-ahead distance L is considered as a monotonic function of vehicle velocity V. Therefore, a driver is assumed to look at the point where the vehicle will pass T_d [s] later, namely $L = T_d V$. T_d is called preview time. [11] indicates that there are upper limit of the steering gain h and lower one of the preview time T_d for operating vehicles stably.

D. Quantitative evaluation method of steering stability

The objective of this paper is to propose the method for finding optimal parameters of YMO in order to improve steering stability in simulations. In this section, therefore, the quantitative evaluation method of steering stability is proposed.

For evaluating steering stability, the following factors need to be taken into consideration.

- High tracking performance to the target course.
- Decreasing δ_f as much as possible to reduce driver stress.
- Decreasing $\dot{\delta}_f$ as much as possible to improve comfort.

To satisfy these requirements, two evaluation indicators are proposed as follows.

- Average difference : the area between the target course and the actual trajectory, divided by total length.
- Total steering amount : the total area of lissajous curve between δ_f and $\dot{\delta}_f$.

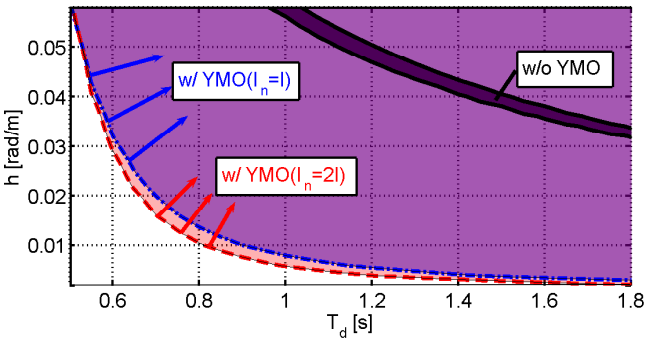

Fig. 9. Simulation results of disturbance suppression (stable area).

If these indicators are both small, the driver is regarded to have operated the vehicle stably.

Since drivers' steering gain h and preview time T_d are assumed to be different among individuals, average difference and total steering amount are calculated with variable h and T_d. Then upper limitations are made both on the average difference and on the total steering amount. The contour line with x-axis T_d and y-axis h can be plotted to meet both limitations. In this paper, the area within this line is defined as stable area, and the larger the area is, the more drivers can operate the vehicle stably.

V. Simulation

A. Disturbance suppression on a straight road

When lateral wind acts on a vehicle running straight at high speed, for example, on an expressway, lateral force and yaw-moment are generated at and around the center of mass [10]. The simulation assumes a lateral force disturbance of $Y_d = 800$ [N] and a yaw-moment of $N_d = 400$ [Nm] from 1 to 2 [s] while running straight at $V = 100$ [km/h]. Then simulation results are compared in three situations — without YMO, and with YMO ($I_n = I, 2I$). The other parameters are $\omega_c = 10$ [rad/s], $\tau_\gamma = 0.15$ [s], $K_{\mathrm{YMO}} = 0.9$.

Fig. 9 shows the simulation result of the stable areas as the average difference is less than 0.1 [m] and the total steering amount less than 0.01 [rad^2/s]. The stable area greatly widens with YMO and, in addition, slightly widens when $I_n = 2I$ in comparison to when $I_n = I$. Therefore, when running straight at high speed, drivers can operate vehicles more stably with YMO, and stability ban be improved by setting I_n higher than the actual value.

Fig. 10 shows an example of results when $h = 0.02$ [rad/m], $T_d = 1.3$ [s]. In Fig. 10(c), the ability to run straight is improved as disturbance is suppressed by yaw-moment N_z generated by in-wheel motors. Compared to the result of $I_n = I$, driver's steering angle δ_f slightly decreases in $I_n = 2I$ as shown in Fig. 10(a).

B. Changing of steering performance

In this section, the effect of varying τ_γ on steering stability and handling is considered. For the test, drivers are told to perform a double-lane-change, as shown in Fig. 11. Such test procedures are given in ISO, which are usually carried out in the vicinity of 100 [km/h]. In this paper, however, the test is conducted in the precinct of the university, thus the vehicle speed is limited to 15 [km/h].

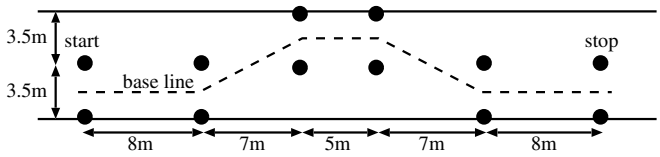

Fig. 11. Test course.

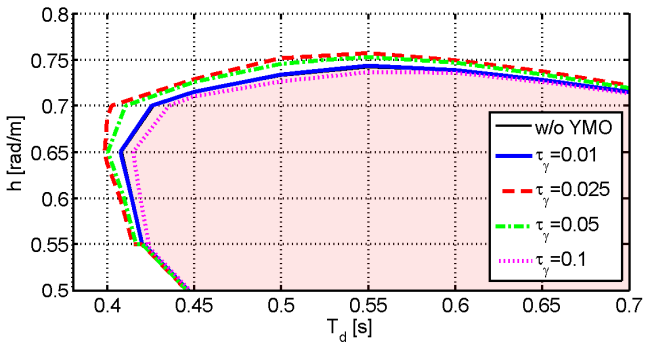

Fig. 12. Simulation results of double-lane-change (stable area).

In the simulation, the target course for the driver model is given as the base line, the broken line in Fig. 11. The average difference is calculated by the distance between the base line and the vehicle trajectory. The parameters are $\omega_c = 10$ [rad/s], $K_{\mathrm{YMO}} = 0.9$, and the mechanical limitation from -0.5 to 0.5 [rad] is imposed on δ_f. At $V = 15$ [km/h], yaw response time from δ_f to γ of "FPEV2-Kanon" is about 0.05 [s].

Simulation results are obtained under five situations and compared — without YMO, with YMO (τ_γ = 0.01, 0.025, 0.05, 0.1 [s]). Fig. 12 shows the simulation results of the stable areas when the average difference is less than 0.1 [m] and the total steering amount less than 1.5 [rad^2/s]. In general, low τ_γ makes a vehicle easy for drivers to operate because of little response delay. However, Fig. 12 shows that the stable area is the broadest when $\tau_\gamma = 0.025$ [s], and comparatively narrow as without YMO when $\tau_\gamma = 0.01$ [s]. These results shows that the decrease of γ_τ does not always lead to the improvement of steering stability for drivers who have short preview time T_d and large steering gain h.

VI. Experiment

A. Disturbance suppression on the straight road

In the precinct of the university, it is difficult to perform high-speed tests or to obtain side disturbance by natural wind. Therefore, a virtual equivalent yaw-moment disturbance is generated by driving and braking force differences of rear motors and rear steering angle by rear EPS. Then it can be

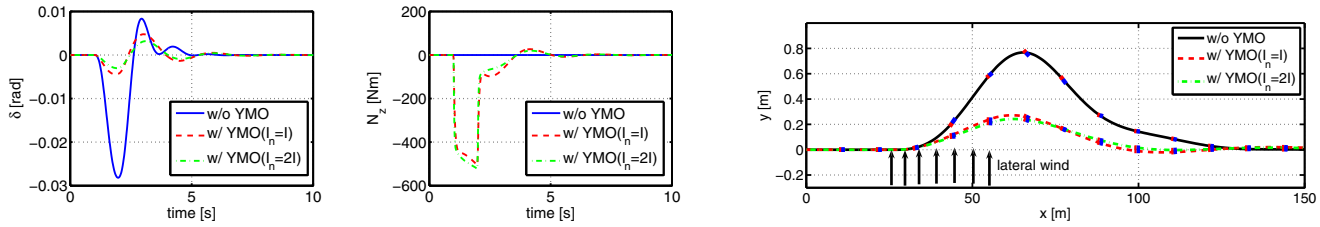

(a) δ_f. (b) N_z. (c) Trajectory.

Fig. 10. Simulation results of disturbance suppression ($h = 0.02$, $T_d = 1.3$).

confirmed by experiments whether disturbance and driver's steering angle is suppressed by YMO.

Fig. 13(a) shows the generated disturbance yaw-moment N_d and rear steering angle δ_r when the vehicle is running straight at 15 [km/h]. N_z, calculated yaw-moment by YMO, is generated by driving and braking force differences of front motors. For reproducibility, steering operation is done by the front EPS whose angle reference is computed by the driver model. The parameters are $\omega_c = 10$ [rad/s], $\tau_\gamma = 0.05$ [s], $K_{\mathrm{YMO}} = 0.9$, $h = 0.1$ [rad/m], $T_d = 1.0$ [s].

Fig. 13 shows the experimental results. Fig. 13(b) and Fig. 13(c) shows that yaw-rate γ caused by disturbance yaw-moment is suppressed by driving and braking force differences. Steering angle decreases as shown in Fig. 13(d) and straightness of vehicle trajectory improves as shown in Fig. 13(e). Additionally, compared to the case of $I_n = I$, steering angle reduces in the case of $I_n = 1.4I$.

Fig. 13(b), however, shows that N_z oscillates when $I_n = 1.4I$. For analyzing this phenomenon, the open-loop transfer function $G_{\gamma N_z}(s)$ from N_z to γ is as follows:

$$G_{\gamma N_z}(s) = \frac{I_n \omega_c[(1 + K_{\mathrm{YMO}})s + \omega_c]}{Is[s + (1 - K_{\mathrm{YMO}})\omega_c]}. \tag{11}$$

The upper limit of dead time in each value of I_n, can be calculated as $T = \theta_m/\omega_p$, where θ_m is the phase margin and ω_p is the frequency in which the gain is 0 [dB]. Fig. 14 is the plot with x-axis I_n/I and y-axis T, which shows that the robustness against the dead time decreases in proportion to the increase of I_n. Therefore, in practice, I_n has an upper limit to be fixed due to sensor delays, response lag due to vehicle mechanical dynamics and other reasons, which aren't taken into consideration in simulations.

B. Sensory test in changing of steering performance

In Sec. V-B, the relationships between τ_γ and steering stability is discussed by simulations. In order to verify the validity of this result, a sensory test is performed. In this test, drivers are directed to drive the experimental vehicle "FPEV2-Kanon" along the course shown in Fig. 11, then it is examined how the feeling of driving changes by the variation of τ_γ.

The following are the contents of the test. The drivers are 8 persons who have been driving for 4-20 years constantly, and all of them do not have experiences of driving the experimental vehicle. Cones are placed on the black circles in Fig. 11,

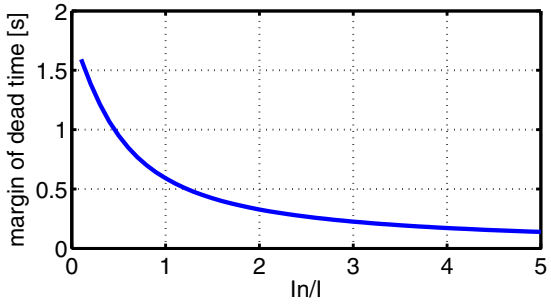

Fig. 14. Upper limit of dead time.

then the drivers are asked to accelerate until $V = 15$ [km/h] and to pass between each two cones. The steering wheel of the vehicle is extremely heavy and hard to drive compared to ordinary vehicles because it does not have steering assist system. Therefore, in order to become used to operating the vehicle, firstly the drivers perform the test twice without YMO, namely without the driving and breaking force difference. Then they drive three times with YMO, for three different values of τ_γ: 0.01, 0.025, 0.1 [s]. After each test, they are asked to answer the questionnaire — lightness of steering (1:heavy - 5:light), speed of response (1:slow - 5:fast), and vehicle handling (1:hard - 5:easy) — regarding 3 as the feeling without YMO.

The bar graph Fig. 15 shows the result of the questionnaire, each bar representing the average of answers with error bars representing standard deviation. In this graph, lightness of steering increases as τ_γ gets small. This is assumed to be because with low τ_γ, yaw-moment N_z is generated by the driving and breaking force difference in the same direction as steering angle for making the vehicle's response speed faster than the actual one.

As for handling, the result is higher than 3 for $\tau_\gamma = 0.025$ [s], which means the vehicle is easier to drive with YMO enabled. For $\tau_\gamma = 0.01$ [s], on the other hand, the result is lower than 3. This results shows that setting τ_γ low does not always improve handling, and there exists an optimal value of τ_γ for improving ease of driving.

VII. Conclusion

In this paper, a design method of Yaw-Moment Observer for improving steering stability and vehicle handling is con-

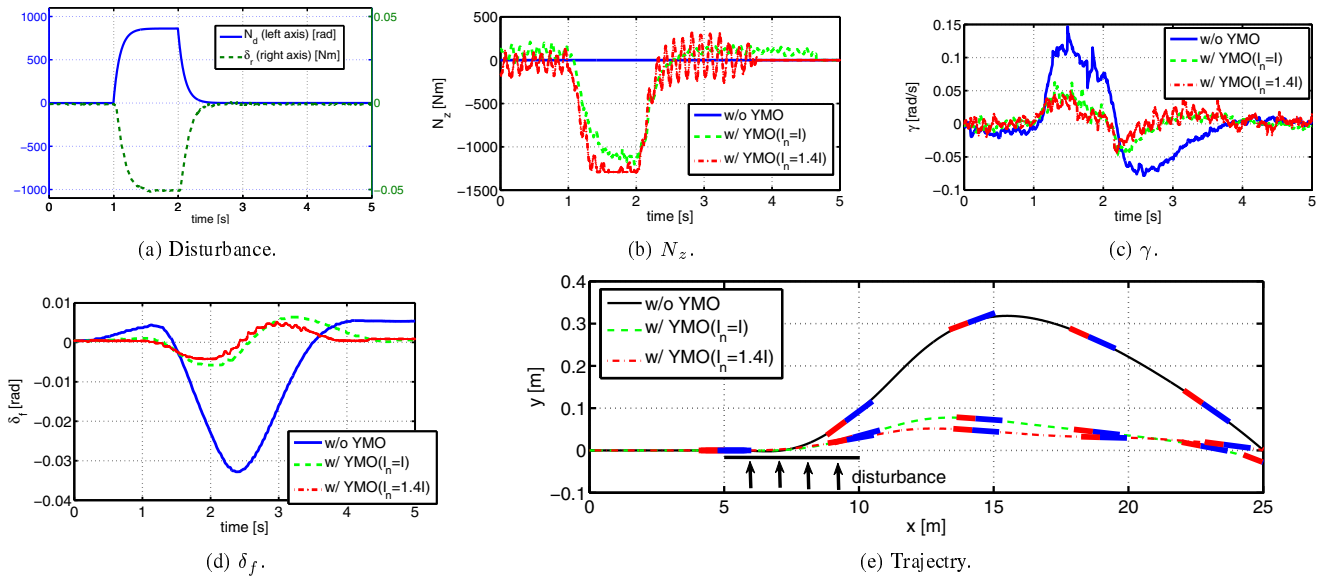

(a) Disturbance. (b) N_z. (c) γ.

(d) δ_f. (e) Trajectry.

Fig. 13. Experimental results of disturbance suppression.

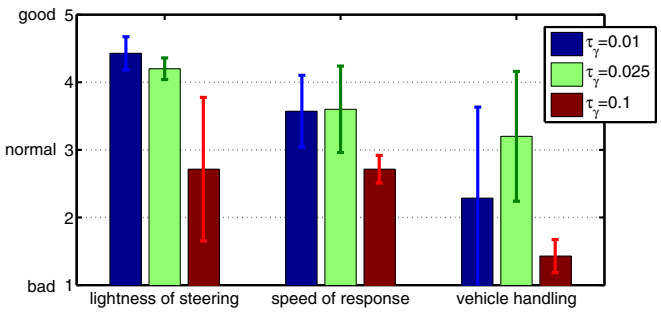

Fig. 15. Result of questionnaire.

sidered. By adopting a driver model, it is verified by both simulations and experiments, that drivers can operate vehicles stably with YMO even in the presence of lateral wind, and that vehicle handling can be improved by changing vehicle characteristics. Moreover, a quantitative evaluation method of steering stability and vehicle handling is proposed and its effectiveness verified by a sensory test.

Future work includes formulation of a method for the optimal design of I_n and τ_γ for improving steering stability, vehicle handling, and comfortability. In addition, the effect of changing K_s and ω_c on steering stability are not considered in this paper, and also forms part of future work.

ACKNOWLEDGMENT

This research was partly supported by the Industrial Technology Research Grant Program from the New Energy and Industrial Technology Development Organization (NEDO) of Japan.

REFERENCES

[1] Y.Hori: "Future vehicle driven by electricity and control—research on four-wheel-motored "UOT Electric March II"", IEEE Trans. on Industrial Electronics, Vol.51, No.5, pp.954-962 (2004)

[2] M.Kamachi, K.Walters: "A research of direct yaw-moment control on slippery road for in-wheel motor vehicle", in Proc. International Battery, Hybrid and Fuel Electric Vehicle Symposium, pp.2122-2133 (2006)

[3] D.Yin, Y.Hori: "A new approach to traction control of EV based on maximum effective torque estimation", Proc. of the 34th Annual Conference of the IEEE Industrial Electronics Society, IECON 2008, pp.2764-2769 (2008)

[4] K.Kawashima, T.Uchida, M.Tomizuka, Y.Hori: "Rolling stability control of in-wheel electric vehicle based on two-degree-of-freedom control", The 10th IEEE International Workshop on Advanced Motion Control 2008, pp.751-756 (2008)

[5] H.Fujimoto, T.Saito, T.Noguchi: "Motion stabilization control of electric vehicle under snowy conditions based on yaw-moment observer", The 8th IEEE International Workshop on Advanced Motion Control 2004, pp.35-40 (2004)

[6] A.H.El-Shaer, M.Tomizuka : "Robust multi-objective control for systems involving human-in-the-loop passivity constraints with application to electric power steering", International Conference on Advanced Intelligent Mechatronics 2010, pp.361-366 (2010)

[7] L.Zhou, L.Ou, C.Wang: "A Simulation of the Four-Wheel Steering Vehicle Stability Based on DYC Control", The International Conference on Measuring Technology and Mechatronics Automation 2009, pp.189-193 (2009)

[8] G.Shu-fang, W.Li-fang: "Strategies to improve steering handling performance for steer-by-wire system", International Conference on Computer and Communication Technologies in Agriculture Engineering 2010, pp.296-299 (2010)

[9] Y.Yamauchi, H.Fujimoto: "Advanced motion control of electric vehicle based on lateral force observer with active steering", 2010 IEEE International Symposium on Industrial Electronics, pp.3627-3632 (2010)

[10] Masato Abe: "Vehicle Handling Dynamics", Butterworth-Heinemann (2009)

[11] T.Fujioka: "Theoretical reserach on the stability of the closed system composed of a look-ahead driver and a planer vehicle" JSAE Annual Congress, No.11-7, pp.29-34 (2007) (in Japanese)